Stem Cell Research 16 (2016) 365–376

Contents lists available at ScienceDirect

Stem Cell Research

journal homepage: www.elsevier.com/locate/scr

Methods and reagents

Development of a cell-defined siRNA microarray for analysis of gene function in human bone marrow stromal cells

Hi Chul Kim [a,c], Gi-Hwan Kim [b], Ssang-Goo Cho [c], Eun Ju Lee [b,*], Yong-Jun Kwon [a,**,1]

[a] Institut Pasteur Korea, IP-Korea, 696 Sampyeong-dong, Bundang-gu, Seongnam-si, Gyeonggi-do, 463-400, Republic of Korea
[b] Biomedical Research Institute and IRICT, Seoul National University Hospital, Seoul, Republic of Korea
[c] Department of Animal Biotechnology (BK21), Animal Resources Research Center, Konkuk University, Seoul 143-702, Republic of Korea

ARTICLE INFO

Article history:
Received 31 August 2015
Received in revised form 24 December 2015
Accepted 6 February 2016
Available online 10 February 2016

Keywords:
Cell-defined siRNA microarray
Cell spot system
Human bone marrow stromal cells
Small scale
siRNA screening

ABSTRACT

Small interfering RNA (siRNA) screening approaches have provided useful tools for the validation of genetic functions; however, image-based siRNA screening using multiwell plates requires large numbers of cells and time, which could be the barrier in application for gene mechanisms study using human adult cells. Therefore, we developed the advanced method with the cell-defined siRNA microarray (CDSM), for functional analysis of genes in small scale within slide glass using human bone marrow stromal cells (hBMSCs).

We designed cell spot system with biomaterials (sucrose, gelatin, poly-L-lysine and matrigel) to control the attachment of hBMSCs inside spot area on three-dimensional (3D) hydrogel-coated slides. The p65 expression was used as a validation standard which described our previous report. For the optimization of siRNA mixture, first, we detected five kinds of commercialized reagent (Lipofectamine 2000, RNAi-Max, Metafectine, Metafectine Pro, TurboFectin 8.0) via validation. Then, according to quantification of p65 expression, we selected 2 μl of RNAi-Max as the most effective reagent condition on our system. Using same validation standard, we optimized sucrose and gelatin concentration (80 mM and 0.13%), respectively. Next, we performed titration of siRNA quantity (2.66–5.55 μM) by reverse transfection time (24 h, 48 h, 72 h) and confirmed 3.75 μM siRNA concentration and 48 h as the best condition. To sum up the process for optimized CDSM, 3 μl of 20 μM siRNA (3.75 μM) was transferred to the 384-well V-bottom plate containing 2 μl of dH_2O and 2 μl of 0.6 M sucrose (80 mM). Then, 2 μl of RNAi-Max was added and incubated for 20 min at room temperature after mixing gently and centrifugation shortly. Five microliters of gelatin (0.26%) and 2 μl of growth factor reduced phenol red-free matrigel (12.5%) were added and mixed by pipetting gently. Finally, optimized siRNA mixture was printed on 3D hydrogel-coated slides and cell-defined attachment and siRNA reverse transfection were induced.

The efficiency of this CDSM was verified using three siRNAs (targeting p65, Slug, and N-cadherin), with persistent gene silencing for 5 days. We obtained the significant and reliable data with effective knock-down in our condition, and suggested our method as the qualitatively improved siRNA microarray screening method for hBMSCs.

1. Introduction

RNA interference (RNAi), which induces the knockdown of specific genes by binding to complementary sequences of mRNA transcripts to promote mRNA degradation, was first developed for post-transcriptional silencing in *Caenorhabditis elegans*. Since then, RNAi screening has been used as a tool for functional genomic studies in mammalian cells. RNAi screening facilitates the identification of genes associated with a given pathway by silencing specific genes and has been shown to have applications in a variety of fields, including cell signaling, cancer, and infectious disease (Seyhan and Ryan, 2010; Cherry, 2009; Fire et al., 1998; Iorns et al., 2008; Luo et al., 2009; Prudêncio and Lehmann, 2009; Scholl et al., 2009).

Reverse transfection cell microarrays have been developed as a new high-throughput system following the reporting of the lipid-DNA method (LDM) (Wheeler et al., 2005; Stürzl et al., 2008; Kittler et al., 2007; Genovesio et al., 2011a, 2011b; Erfle et al., 2007; Castel et al., 2006; Stürzl et al., 2008; Ziauddin and Sabatini, 2001). This method allows for reduced screening time, rapid analysis, and visualization of cell phenotype and is therefore advantageous over more traditional screening methods. Moreover, many investigators have adapted this concept to

* Correspondence to: E. J. Lee. Biomedical Research Institute and IRICT, Center for Cell and Gene Therapy, Seoul National University Hospital, 101 Daehak-ro, Jongro-gu, Seoul 110-744, Republic of Korea.
** Correspondence to: Y. J. Kwon. Ksilink, 16 Rue d'Ankara, Strasbourg 67000, France.
E-mail addresses: leeunju@snu.ac.kr (E.J. Lee), yjkwonipk@gmail.com (Y.-J. Kwon).
[1] Current address: Ksilink, 16 Rue d'Ankara, Strasbourg 67000, France.

http://dx.doi.org/10.1016/j.scr.2016.02.019

siRNA microarray platforms for further development by using different cell types and various transfection reagents, such as Lipofectamine 2000, lipofectin, effectene, and culture surfaces coated with amino silane (GAPS) and poly-L-lysine (PLL) (Erfle et al., 2007; Baghdoyan et al., 2004; Kumar et al., 2003; Mousses et al., 2003; Redmond et al., 2004; Silva et al., 2004; Webb et al., 2003). We also developed an siRNA microarray system using Lipofectamine 2000 and PLL-coated coverslips for automated genome-wide visual profiling of cellular proteins involved in human immunodeficiency virus (HIV) infections and identification of human-host factors associated with *Trypanosoma cruzi* infection (Genovesio et al., 2011a, 2011b). However, in these siRNA microarrays, siRNA spreading between spot and spot is observed in cells that exhibit mobility, such as human bone marrow stromal cells (hBMSCs), which have an elongated cell shape and show high migration activity (Supplemental Fig. 1). In addition to these limitations, it is also difficult to obtain sufficient numbers of hBMSCs for high-throughput screening assays. Therefore, despite the necessity for additional studies of the functions of genes in hBMSCs, siRNA microarrays or similar methods are not commonly used for functional genomics studies.

In this study, we present the other method, the cell-defined siRNA microarray (CDSM), which was designed to restrict the culture of hBMSCs inside the spot area without reducing the efficiency of siRNA silencing. This CDSM technology may be applicable for functional genomic studies with limited numbers of cells and is expected to provide efficient method for siRNA screening.

2. Materials and methods

2.1. hBMSCs culture

hBMSCs were purchased from Lonza (Basel, Switzerland). The cells were cultured in MSC basal medium (MSCBM; Lonza), supplemented with BMSC growth medium (MSCGM), an hBMSCs SingleQuots kit (Lonza), 5% fetal bovine serum, 1% L-glutamine, and 0.1% GA-1000. Cultures were maintained at 37 °C in a humidified cell incubator with an atmosphere of 5% CO_2, and the culture medium was changed twice per week.

2.2. Optimization of the siRNA solution

We used p65 protein expression, a component of the NF-kB complex, as validation control because its silencing could be easily estimated by immunofluorescence staining (Genovesio et al., 2011b), and confirmed p65 protein expression of hBMSCs before optimization of CDSM. The basic mixing method for the siRNA solution was described previously (Genovesio et al., 2011a, 2011b; Rantala et al., 2011). For biomaterials selection, 2 μl of 20 μM scramble siRNA, 2.66 μM as final concentration, was transferred to the 384-well V-bottom plate (Greiner Bio-one) containing 0 μl to 7 μl of dH_2O with 2 μl of 0.8 M sucrose, 106 mM as final concentration (Invitrogen, Carlsbad, CA, USA) diluted in Opti-MEM (Gibco, USA) or without sucrose following conditions. Two microliters of Lipofectamine 2000 was added and the solution was mixed gently. The complexes of siRNA and transfection reagent were incubated for 20 min at room temperature after centrifugation (1200 rpm, 30 s). Five microliters of gelatin (diluted in dH_2O, 0.26% final concentration; Invitrogen) and 2 μl of PLL (diluted in dH_2O, 0.0053% final concentration; Sigma) were added; not following conditions, 2 μl of growth factor reduced phenol red-free matrigel (BD Biosciences, USA) was added; or not following conditions, all solution was mixed by pipetting. The detailed information such as final concentration was summarized in Table 1.

For the selection of transfection reagent, 2 μl of 20 μM siRNA, 2.66 μM as final concentration (scramble and p65 siRNA as a smart pool of four individual siRNAs per target; Dhamacon) was transferred to the 384-well V-bottom plate (Greiner Bio-one) containing 2 μl of dH_2O and 2 μl of 0.8 M sucrose, 106 mM as final concentration (Invitrogen, Carlsbad, CA, USA) diluted in Opti-MEM (Gibco, USA). Each 2 μl of transfection reagents (Lipofectamine 2000, RNAi-Max [Invitrogen, USA]; Metafectine, Metafectine Pro [Biontex, Germany], and TurboFectin 8.0 [OriGene, USA]) was added, and the solution was mixed gently. The complexes containing siRNA and transfection reagent were incubated for 20 min at room temperature after centrifugation (1200 rpm, 30 s). Five microliters of gelatin (diluted in dH_2O, 0.26% final concentration; Invitrogen) and 2 μl of growth factor reduced phenol red-free matrigel (BD Biosciences, USA) were added and mixed gently by pipetting.

For the validation of transfection reagent volume, 2 μl of 20 μM scramble and p65 siRNA (2.5 μM, 2.66 μM and 2.85 μM as final concentration) was transferred to the 384-well V-bottom plate containing 2 μl of dH_2O and 2 μl of 0.8 M sucrose (100 mM, 106 mM and 114 mM as final concentration) diluted in Opti-MEM. Each 3 μl, 2 μl and 1 μl of RNAi-Max was added and then the solution was mixed gently. The complexes containing siRNA and transfection reagent were incubated for 20 min at room temperature after centrifugation (1200 rpm, 30 s). Five microliters of gelatin diluted in dH_2O (0.25%, 0.26% and 0.28% as final concentration; Invitrogen) and 2 μl of growth factor reduced phenol red-free matrigel (BD Biosciences, USA) were added and mixed gently by pipetting.

For the validation of sucrose and gelatin, 2 μl of 20 μM scramble and p65 siRNA (2.66 μM as final concentration) was transferred to the 384-well V-bottom plate containing 2 μl of dH_2O and each 2 μl of 1.6 M, 0.8 M and 0.6 M sucrose (213 mM, 106 mM and 80 mM as final concentration) diluted in Opti-MEM. Two microliters of RNAi-Max was added and then the solution was mixed gently. The complexes containing siRNA and transfection reagent were incubated for 20 min at room temperature after centrifugation (1200 rpm, 30 s). Five microliters of 0.8% and 0.4% gelatin diluted in dH_2O (0.26% and 0.13% as final concentration) and 2 μl of growth factor reduced phenol red-free matrigel (BD Biosciences, USA) were added and mixed gently by pipetting.

For the validation of siRNA volume and reverse transfection time, each 2 μl to 5 μl of 20 μM scramble and p65 siRNA (2.66 μM, 3.75 μM, 4.7 μM and 5.55 μM as final concentration) was transferred to the 384-well V-bottom plate containing 2 μl of dH_2O and each 2 μl of 0.6 M sucrose (80 mM, 75 mM, 70.58 mM and 66.66 mM as final concentration) diluted in Opti-MEM. Two microliters of RNAi-Max was added and then the solution was mixed gently. The complexes containing siRNA and transfection reagent were incubated for 20 min at room temperature after centrifugation (1200 rpm, 30 s). Five microliters of 0.4% gelatin diluted in dH_2O (0.13%, 0.12% and 0.11% as final concentration) and 2 μl of growth factor reduced phenol red-free matrigel (BD Biosciences, USA) were added and mixed gently by pipetting.

After each all step, the solution was mixed gently and centrifuged (1200 rpm, 30 s). The summarized information was shown in Table 2.

2.3. Printing for CDSM

Three-dimensional (3D) hydrogel-coated slides (H; 25 × 75.6 × 1 mm; SCHOTT) were held at room temperature for 30 min to 1 h before opening the packaging bag; this step is very important for achieving quality microarray results because chilled slides generate moisture on the surface, leading to fur forms. The prepared siRNA transfection solution was printed on the 3D hydrogel-coated slide using SMP9 stealth pins (Telechem, Atlanta, GA, USA) and a high-throughput microarray printer (Genomic Solutions, Ann Arbor, MI, USA) at 22–25 °C and 55–60% relative humidity. Printed spots were 250–350 μm in diameter with a 700 μm spot-to-spot interval. The prepared CDSMs were dried in a desiccating chamber overnight, packaged in airtight bags, and then stored at 4 °C until further use.

2.4. hBMSCs preparation and culture on the CDSMs

Vials of hBMSCs stored in liquid nitrogen (LN_2) tank were thawed in 25 T or 75 T flasks and then cultured for 1 week to reach 70%–80%

confluence. The prepared cells (2×10^5 cells/4 ml/slide) detached by incubation with 0.05% trypsin–EDTA (Gibco) were seeded on CDSMs which were removed from moisture and transferred to a 4-well rectangular dish (Nunc, USA). Cell attachment was induced for 10 min, and unattached cells were removed by washing 3–5 times with fresh hBMSCs medium. Even after incubation of unattached cells for more than 24 h without washing, no cell attachment was observed on the slide surface outside of the spots (data not shown). The hBMSCs attached on the spot region were cultured for 1–7 days to induce reverse transfection. The medium was refreshed every 48 h.

2.5. Immunofluorescence staining

The immunofluorescence staining of hBMSCs on CDSMs was performed using standard methods. The cells were washed with 1× phosphate-buffered saline (PBS) once and fixed with 4% (*w*/*v*)

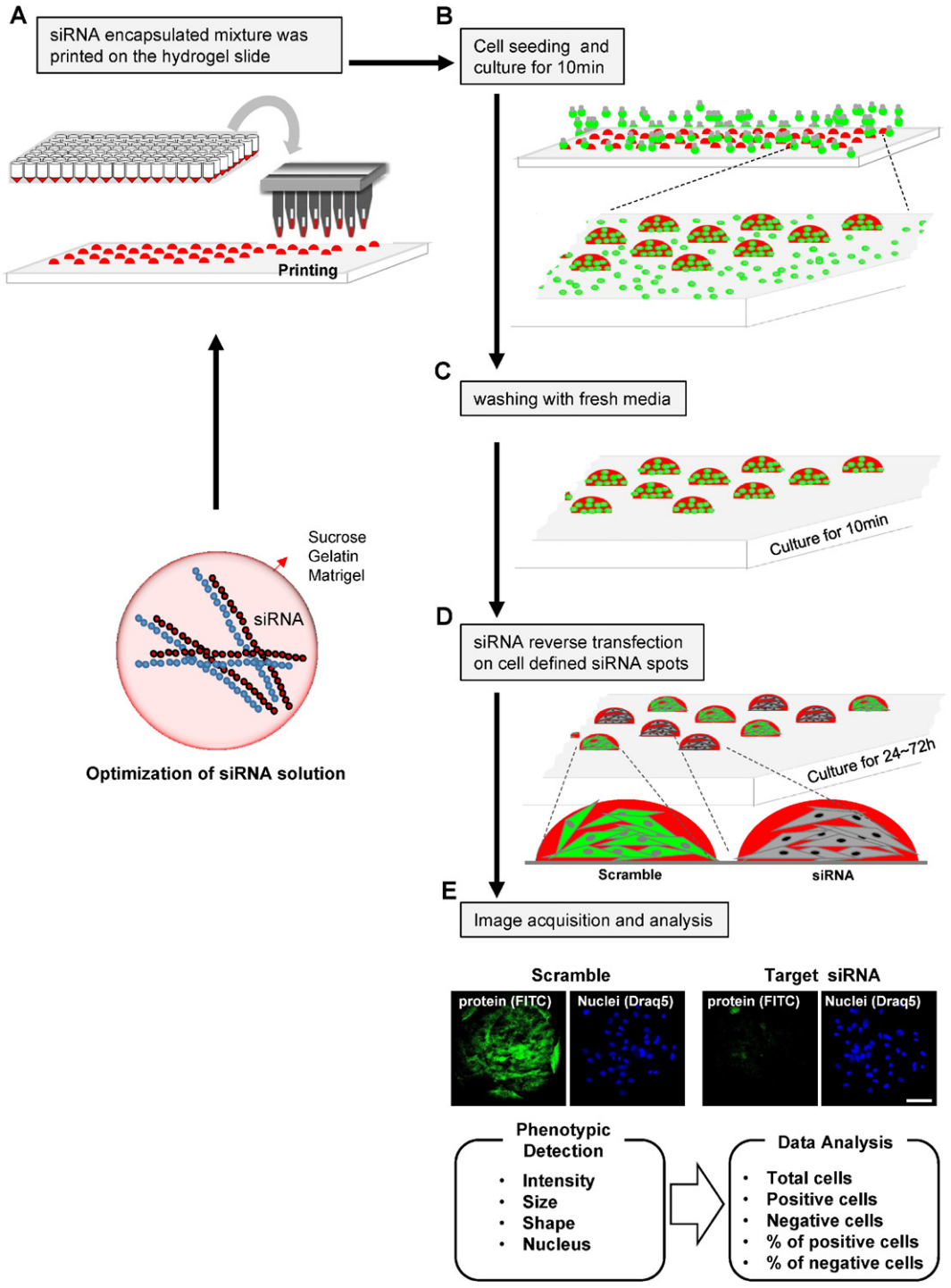

Fig. 1. Schematic of the development of the hBMSCs microarray. (A) Printing of the optimal siRNA solution using a high-throughput microarray printer on 3D hydrogel-coated slides. (B) Seeding and culture for 10 min to induce attachment of cells on the spots. (C) Removal of unattached cells by washing gently with fresh media. (D) The delivery of siRNA into the spot-cultured hBMSCs. (E) Image acquisition and analysis using an ImageXpress Ultra Point scanning confocal microscope and MetaXpress software. The image of the cell spots was acquired with two fluorescent channels, which were filtered with Alexa 488 for green fluorescence and 635 nm for Draq5. The image was analyzed by measurement of the proportion of fluorescently stained cells, which was calculated by measuring the fluorescence intensity, cell number, and cell size.

paraformaldehyde in 1× PBS for 10 min. Cells were then washed again with 1× PBS and permeabilized with 0.001% Triton-X100 in 1× PBS for 10 min. Primary antibodies targeting CD105 (1:200 dilution; mouse monoclonal; Santa Cruz Biotechnology, CA, USA), CD29 (1:100 dilution; mouse monoclonal; Merck Millipore), CD14 (1:200 dilution; mouse monoclonal; Santa Cruz Biotechnology, CA, USA), CD34 and CD45 (1:200 dilution; rabbit polyclonal; Santa Cruz Biotechnology, CA, USA), p65 (1:400 dilution; rabbit polyclonal; Santa Cruz Biotechnology), Slug (1:200 dilution; rabbit monoclonal; Cell Signaling Technology, Beverly, MA, USA), N-cadherin (1:1600 dilution; mouse monoclonal; Santa Cruz Biotechnology), β-catenin (1:100 dilution; rabbit monoclonal; Cell Signaling Technology), normal mouse and rabbit IgG (1;100 dilution; unconjugated, affinity purified isotype control immunoglobulin from mouse and rabbit; Santa Cruz Biotechnology) were diluted with 10% goat serum in 1× PBS. Primary antibodies targeting CD73 (1:200 dilution; goat polyclonal; Santa Cruz Biotechnology) and normal goat IgG (1;100 dilution; unconjugated, affinity purified isotype control immunoglobulin from goat; Santa Cruz Biotechnology) were diluted with 1% bovine serum albumin (BSA) in 1× PBS. All primary antibody incubations were performed for 1.5 h at room temperature. After washing three times with 1× PBS, secondary goat anti-rabbit or goat anti-mouse antibodies conjugated with Alexa 488 were diluted with 10% goat serum in 1× PBS, and donkey anti-goat antibodies conjugated with Alexa 568 were diluted with 1% BSA in 1× PBS (1:1000 dilution; Invitrogen). Secondary antibody incubations were performed for 1.5 h at room temperature. After washing three times with 1× PBS, 5 mM DRAQ5 (1:2000 in PBS;

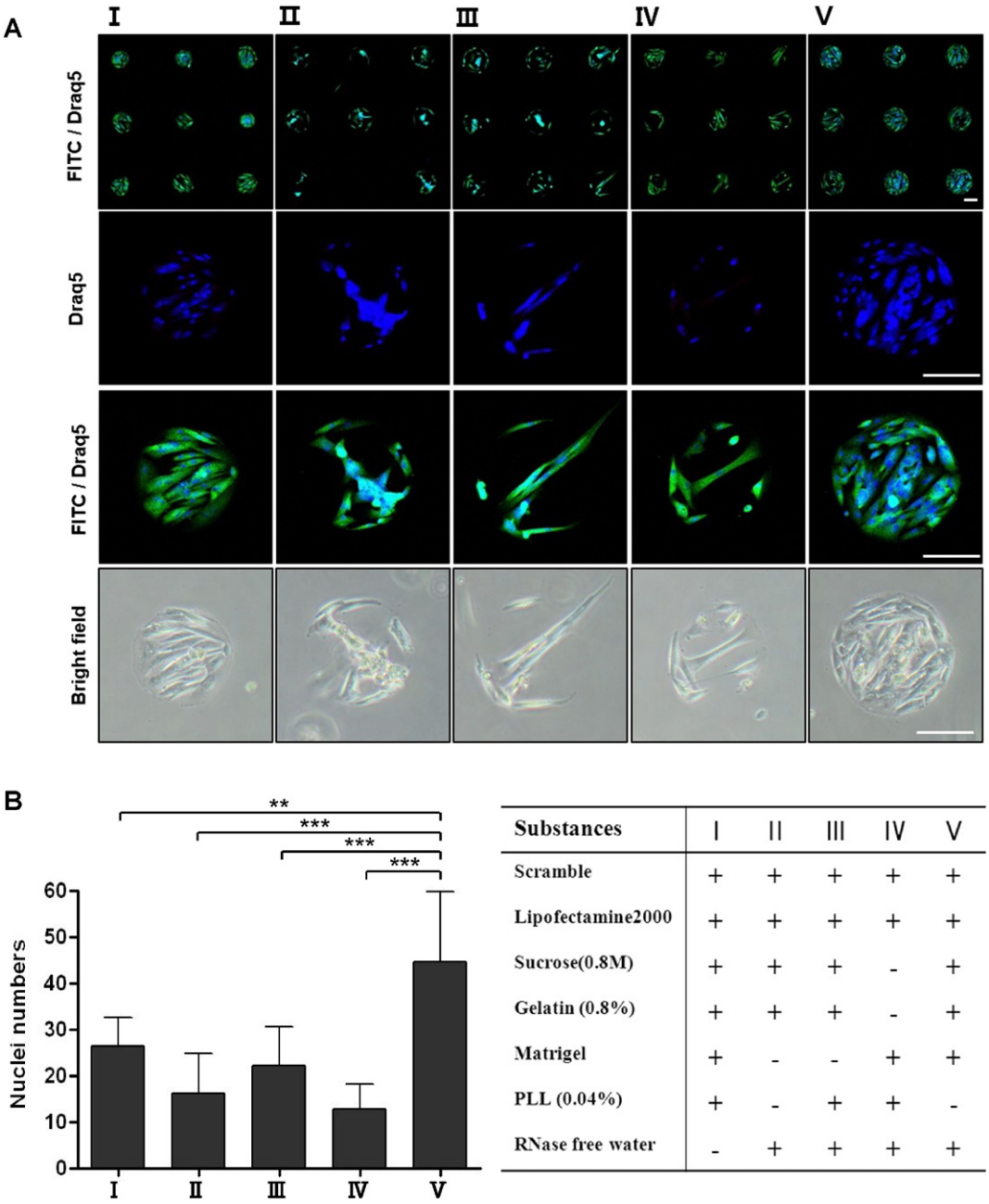

Substances	I	II	III	IV	V
Scramble	+	+	+	+	+
Lipofectamine2000	+	+	+	+	+
Sucrose(0.8M)	+	+	+	-	+
Gelatin (0.8%)	+	+	+	-	+
Matrigel	+	-	-	+	+
PLL (0.04%)	+	-	+	+	-
RNase free water	-	+	+	+	+

Fig. 2. Optimization of biomaterials for the cell-defined array. (A) Immunofluorescence and phase-contrast images of cells cultured for 48 h on scramble siRNA spots, which included various cell-friendly substances. (B) Quantitative analysis of cell numbers in (A) using MetaXpress software and condition of substances solution (right table). The images were obtained using an ImageXpress Ultra Point scanning confocal microscope with anti-p65 antibodies. Blue: nuclei stained with Draq5; green: fluorescently labeled anti-p65 antibodies. Each error bar represents the mean ± SD. $^{**}p < 0.01$, $^{***}p < 0.001$: statistical significance of comparisons between sucrose/gelatin, matrigel medium and others (representative of $n = 9$ array spots, scale bar = 100 μm).

Biostatus, UK) was added, and samples were incubated for 10 min to stain the nuclei. After rinsing with 1× PBS, 2–3 drops of mounting solution (Dako, France) was added to the CDSM, and the slides were covered with glass coverslips (24 × 60 mm; Marienfeld, Germany), ensuring that there were no air bubbles. Slides were then dried for 1 h at room temperature. After fixing with mounting solution, the CDSMs were stored at 4 °C until image acquisition.

2.6. Image acquisition and analysis

Immunofluorescence imaging was performed using an ImageXpress Ultra Point scanning confocal microscope (Molecular Devices, USA) equipped with four solid-state lasers for simultaneous excitation at 405, 488, 561, and 635 nm; a galvanometer for X scanning; and a stage for Y scanning. Each cell spot was scanned at 10× or 20×

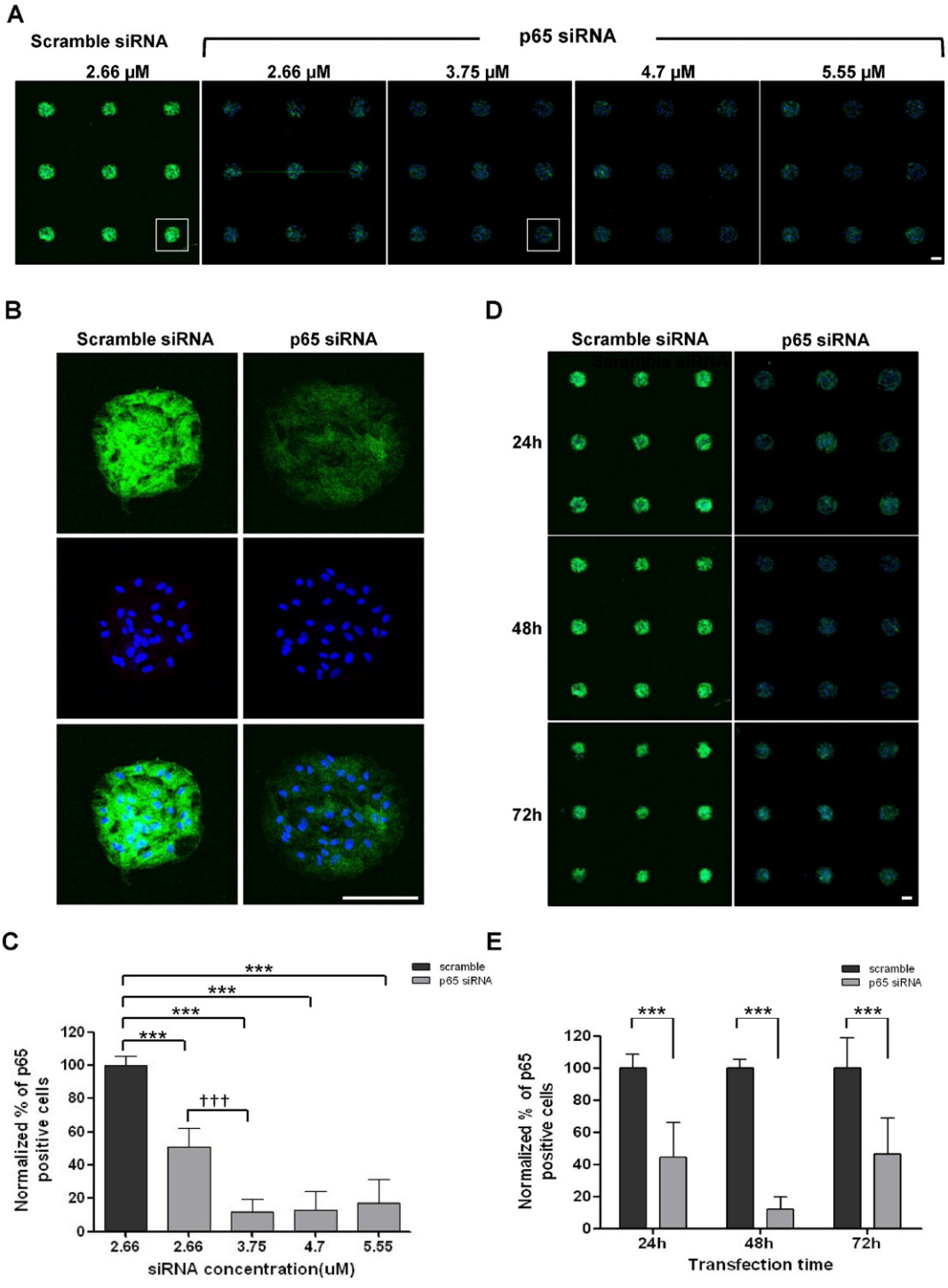

Fig. 3. Selection of optimal siRNA quantity and transfection time. (A) Immunofluorescence image of *p65* gene expression knockdown efficiency according to the concentration of p65 siRNA for 48 h ($n = 9$ array spots, scale bar = 100 μm). (B) Amplified image for cells transfected with 3.75 μM siRNA. (C) Quantitative analysis of the ratio of p65-positive cells in (A). (D) Immunofluorescence image of *p65* gene expression knockdown efficiency according to transfection time ($n = 9$ array spots, scale bar = 100 μm). (E) Quantitative analysis of the ratio of p65-positive cells in (D). Images were obtained using an ImageXpress Ultra Point scanning confocal microscope and anti-p65 antibodies. Blue: nuclei stained with Draq5; green: fluorescently labeled anti-p65 antibodies. Scrambled siRNA was used as a control. The analysis was performed using MetaXpress software. Each error bar represents the mean ± SD. $^{***}p < 0.001$: statistical significance of comparisons with scrambled siRNA; $^{\dagger\dagger\dagger}p < 0.001$: statistical significance of comparisons among p65 siRNA concentrations.

magnification using a Nikon air immersion objective lens with specific filter sets for Alexa488, Alexa568, and Alexa635. The acquired images were analyzed with MetaXpress software (Molecular Devices). Cell scoring parameters were also determined to evaluate the proportion of fluorescent-positive cells, which was calculated according to the fluorescence intensity, nuclei numbers, and size (Fig. 1, Supplemental Fig. 2). GraphPad Prism 5 software was used to determine statistical significance for comparisons of two groups by one-way or two-way analysis of variance (ANOVA) and the Bonferroni method. Differences with p values of less than 0.05 were considered statistically significant.

3. Results

3.1. Establishment of the CDSM

To develop the CDSM, we selected 3D hydrogel-coated slides coated with amine-reactive NHS ester groups as hydrophobic slides with cell-resistant properties. We then attempted to culture hBMSCs on the siRNA spots printed on the slide surface. Because sucrose/gelatin, PLL, and matrigel have been shown to affect the adherence and growth of cells (Genovesio et al., 2011a, 2011b; Rantala et al., 2011), we tested various combinations of these reagents to determine the optimal mixture. Low cell attachment and irregularly shaped cells were observed in culture without sucrose/gelatin or matrigel, and PLL did not significantly influence the adhesion of hBMSCs. Therefore, we chose an appropriate combination of sucrose/gelatin and matrigel for spot-defined hBMSCs attachment and culture (Fig. 2).

We also optimized the transfection reagent for achieving effective siRNA-mediated gene silencing by printing of p65 siRNA solutions combined with different transfection reagents. Three of the reagents showed increased knockdown efficiency of p65 siRNA; RNAi-Max had the most substantial effect among the reagents (Supplemental Fig. 3). For confirmation of the appropriate volume of RNAi-Max, three different volumes (1, 2, and 3 μl) were tested with 2 μl of p65 siRNA (RNAi-Max vs. siRNA, 1 μl vs. 2.85 μM, 2 μl vs. 2.66 μM, 3 μl vs. 2.5 μM). Significant knockdown efficiency was observed at low volumes (i.e., 1–2 μl) when compared with RNAi-Max (3 μl). Therefore, we chose 2 μl of RNAi-Max as the optimum volume because the stability of siRNA knockdown with only 1 μl of RNAi-Max was uncertain (Supplemental Fig. 4A and B).

Sucrose and gelatin are known to be cell-friendly biomaterials; hence, these were used along with matrigel for spot-defined culture (Fig. 2). This combination of sucrose/gelatin and matrigel facilitated cell attachment on the siRNA spot, promoted the formation of circular spots after printing, protected the spots from being washed away by the medium, and influenced the transfection efficiency. However, higher concentrations may cause spreading of spots and ineffective printing due to high viscosity. Moreover, low concentrations sometimes decrease the knockdown efficiency of the siRNA spot. Therefore, we performed experiments to determine the optimal concentrations of sucrose and gelatin. Our results showed that p65 siRNA provided efficient knockdown independent of the concentrations of sucrose and gelatin. Moreover, higher concentrations of sucrose and gelatin (1.6 M/0.8% and 0.8 M/0.8%) caused inefficient printing (with missed spots or variations in spot shape/size). From this analysis, we chose the combination of 0.6 M sucrose and 0.4% gelatin (Supplemental Fig. 4C and E).

For high-efficiency delivery of lipid-based siRNA to cells, the ratio of siRNA to transfection reagent in the mixture is an important factor. From our results described above, we found that 2 μl of RNAi-Max was optimal. Therefore, we next examined the optimal ratio of RNAi-Max to p65 siRNA for various transfection times. The knockdown efficiency of p65 siRNA was significant at all the siRNA concentrations and time conditions except for 2.66 μM p65 siRNA for 72 h. The efficiency was increased dramatically under conditions of more than 3.75 μM siRNA with a 48 h transfection time (Fig. 3, Supplemental Fig. 5).

3.2. Confirmation of hBMSCs localization and characterization on CDSM slides

Next, we confirmed the optimization of the CDSM according to the optimal parameters described above (Figs. 2 and 3, Supplemental Figs. 3–5, Table 1). The characteristics of hBMSCs cultured for 10 min, 1 h, or 48 h on the defined spot areas containing non-targeting siRNA were confirmed. Bright-field images showed that hBMSCs grew and hBMSCs-specific makers were expressed specifically (CD105, CD29, and CD73) or negative expressed (CD14, CD34, and CD45) in hBMSCs (Fig. 4, Supplemental Fig. 6).

3.3. Confirmation of the knockdown efficiency of target genes

For validation of the CDSM, we first attempted to confirm siRNA-mediated knockdown of other target genes that are expressed in hBMSCs. To this end, we examined the knockdown of the nuclear factor (NF) kappa B subunit (p65), the mesenchymal cell maker N-cadherin (NCAD), and the zinc finger transcription factor (Slug) in the newly optimized CDSM. All three genes were significantly down regulated by more than 70% (Fig. 5A-C). To further support the use of CDSM as a tool for functional genomic studies of hBMSCs, we investigated the expression levels of proteins related to NCAD, with a focus on β-catenin, which is involved in the regulation of cell–cell adhesion, gene transcription, and intracellular signal transduction in the Wnt signaling pathway. β-Catenin expression has been shown to be slightly decreased following suppression of N-cadherin expression in HEK293 cells (Howard et al., 2011). Indeed, we found decreased expression of β-catenin on printed N-cadherin siRNA spots on the CDSM (Fig. 5D).

We further examined the knockdown of NCAD by siRNA using a multispot assay developed by printing of a total of 128 spots. All NCAD siRNA spots showed an average of 70% knockdown of NCAD, with approximately 10–15% variation in efficiency. The average number of

Table 1
The condition of printing solution for biomaterials selection.

Substances	Figure				
	Fig. 2-I	Fig. 2-II	Fig. 2-III	Fig. 2-IV	Fig. 2-V
Scramble	2 μl [2.66 μM]	2 μl [2.66 μM]	2 μl [2.66 μM]	2 μl [2.66 μM]	2 μl [2.66 μM]
Lipofectamine2000	2 μl [13.3%]	2 μl [13.3%]	2 μl [13.3%]	2 μl [13.3%]	2 μl [13.3%]
Sucrose (0.8 M)	2 μl [106 mM]	2 μl [106 mM]	2 μl [106 mM]	–	2 μl [106 mM]
Gelatin (0.8%)	5 μl [0.26%]	5 μl [0.26%]	5 μl [0.26%]	–	5 μl [0.26%]
Matrigel	2 μl [13.3%]	–	–	2 μl [13.3%]	2 μl [13.3%]
PLL (0.04%)	2 μl [0.0053%]	–	2 μl [0.0053%]	2 μl [0.0053%]	–
RNase-free water	–	4 μl [26.6%]	2 μl [13.3%]	7 μl [46.6%]	2 μl [13.3%]
Total volume	15 μl	15 μl	15 μl	15 μl	15 μl

( ): Stock concentration.
[ ]: Final concentration. The numbers from second places of decimals are ignored.

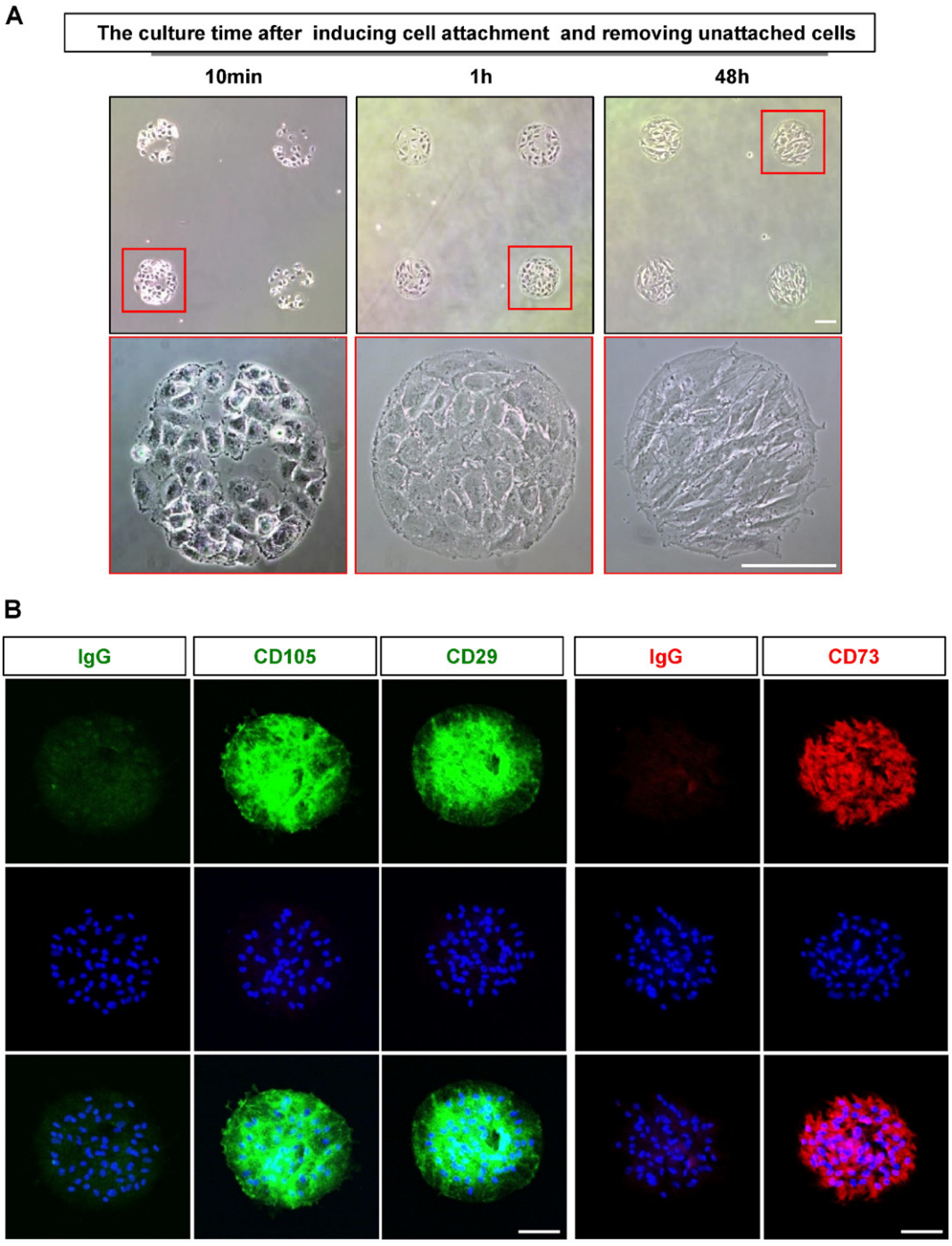

Fig. 4. Characterization of hBMSCs on the siRNA microarray. (A) Phase-contrast cell-spot image after removing unattached cells (representative of $n = 4$ array spots, scale bar = 100 μm). (B) Immunofluorescence image of hBMSCs-specific markers for confirmation of hBMSCs characteristics after 72 h (representative of $n = 4$ array spots, scale bar = 100 μm). The image was obtained using an ImageXpress Ultra Point scanning confocal microscope with anti-CD105, anti-CD29, and anti-CD73 antibodies. Blue: nuclei stained with Draq5; green: fluorescently labeled antibodies targeting CD105 and CD29; red: fluorescently labeled antibodies targeting CD73. Scrambled siRNA was used as a control.

cells in each spot ranged from 30 to 60, and variations in cell numbers did not affect the knockdown efficiency (Fig. 6).

3.4. The persistence of the gene silencing effect on the CDSM

Our data showed that a transfection time of 48 h was sufficient for gene knockdown on the CDSM. However, the persistence of the gene silencing effect is also critical for functional genomics studies, particularly when combining gene knockdown with screening of compounds or inhibitors. Therefore, we examined the efficacy of the siRNA knockdown at 5 days after transfection with p65, Slug, and NCAD siRNAs. We confirmed the inhibition efficacy after 5 days (Fig. 7), although the effect is some decrease comparing with 48 h (Fig. 5 vs. 7; p65 12 vs. 32, Slug 9 vs. 43, N-cadherin 24 vs. 29 respectively). Also the silencing effect of p65 siRNA persisted for 7 days though the efficiency was dramatically decreased (data not shown). These data suggested that the siRNA

Table 2
The work flow of printing solution condition for siRNA reverse transfection optimization.

Processing step	Condition							
	Volume of siRNA (concentration)	Kind of transfection reagent/volume	Volume of sucrose (M) /gelatin (%)	Volume of Matrigel[a]	Volume of RNase-free water[a,b]	The time of reverse transfection	Final confirmed optimization condition	Reference
Selection of transfection reagent	2 μl [2.66 μM] (20 μM)	Lipofectamine 2000, Metafectene, Metafectene PRO, Turbofectine 8.0, RNAi Max. /2 μl	2 μl (0.8 M)/5 μl (0.8%) [106 mM]/[0.26%]	2 μl	2 μl	48 h	RNAi-Max	Suppl. Fig. 3
Validation of transfection reagent volume	2 μl (20 μM) [2.5 μM] vs. 16 μl total vol. [2.66 μM] vs. 15 μl total vol. [2.85 μM] vs. 14 μl total vol.	RNAi-Max/3 μl, 2 μl, 1 μl	2 μl (0.8 M)/5 μl (0.8%) [100 mM]/[0.25%] vs. 16 μl total vol. [106 mM]/[0.26%] vs. 15 μl total vol. [114 mM]/[0.28%] vs. 14 μl total vol.	2 μl	2 μl	48 h	2 μl RNAi Max	Suppl. Fig. 4A and B
Validation of sucrose and gelatin	2 μl [2.66 μM] (20 μM)	RNAi-Max/2 μl	2 μl (1.6 M) [213 mM]/5 μl (0.8%) [0.26%] 2 μl (0.8 M)[106 mM]/5 μl (0.8%) [0.26%] 2 μl (0.6 M)[80 mM]/5 μl (0.8%) [0.26%] 2 μl (0.6 M)[80 mM]/5 μl (0.4%) [0.13%]	2 μl	2 μl	48 h	Sucrose: 2 μl (0.6 M)[80 mM] Gelatin: 5 μl (0.4%) [0.13%]	Suppl. Fig. 4C and D
Validation of siRNA volume and reverse transfection time	2 μl [2.66 μM], 3 μl [3.75 μM] 4 μl [4.7 μM], 5 μl [5.55 μM] (20 μM)	RNAi-Max/2 μl	2 μl (0.6 M)/5 μl (0.4%) [80 mM]/[0.13%] vs. 15 μl total vol. [75 mM]/[0.12%] vs. 16 μl total vol. [70.58 mM]/[0.11%] vs. 17 μl total vol. [66.66 mM]/[0.11%] vs. 18 μl total vol.	2 μl	2 μl	24 h 48 h 72 h	siRNA : 3 μl [3.75 μM] Transfection time: 48 h	Fig. 3 Suppl. Fig. 5

( ): Stock concentration.
[ ]: Final concentration. The numbers from second places of decimals are ignored.
[a] The volume of Matrigel and RNase-free water is fixed.
[b] RNase-free water is just used for total volume.

activity on CDSM was optimal at 48 h after transfection and the activity was detectable until 7 days but it is not recommendable time for effective screening.

Finally, we examined the effects of storage time on the CDSM. Knockdown efficiency was maintained, albeit with a decrease over time, for siRNA spots on CDSMs that were stored for 10 days to 2 months at 4 °C (data not shown).

4. Discussion

Gene or protein chips are common methods used for analyzing the regulation of gene expression, genetic networks, and their pathways. However, the quantity of mRNA often does not reflect the expression of the proteins they correspond to, and the change of the expression in protein often does not induce from mRNA.

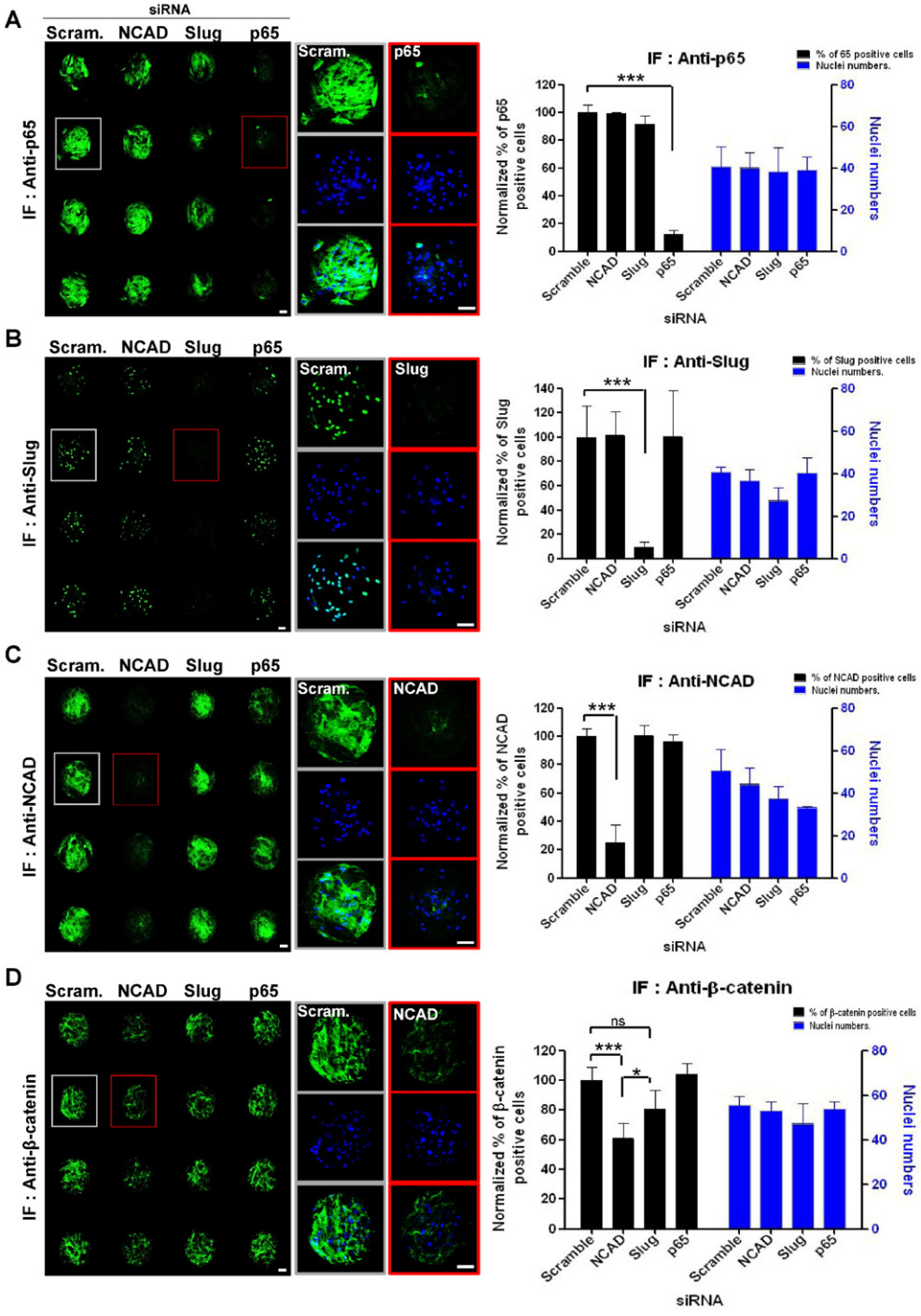

Fig. 5. Effective inhibition of target genes after 48 h transfection in hBMSCs. (A) Anti-p65 labeled immunofluorescence image for the confirmation of p65 protein decrease by p65 siRNA and quantitative analysis of the ratio of p65-positive cells. (B) Anti-Slug labeled immunofluorescence image and quantitative analysis of decreased slug protein. (C) Anti-NCAD labeled immunofluorescence image and quantitative analysis of decreased expression of NCAD protein. (D) Anti-β-catenin labeled immunofluorescence image of decreased β-catenin expression by NCAD siRNA, and quantitative analysis of the ratio of β-catenin-positive cells. The image was obtained using an ImageXpress Ultra Point scanning confocal microscope. Blue: nuclei stained with Draq5; green: fluorescently labeled antibodies against target proteins. Scrambled siRNA was used as a control. The analysis was performed using MetaXpress software. Each error bar represents the mean ± SD. $^{*}p < 0.05$, $^{***}p < 0.001$: statistical significance of comparisons with scramble siRNA ($n = 6$ array spots, scale bar = 100 μm).

Therefore, in this study, we developed the CDSM method that hBMSCs were attached to printed spots and evaluated knockdown of target genes using the expression of the protein. This method is expected to have applications in genome-wide loss-of-function.

Cell-based siRNA microarrays have made it possible to analyze phenotypic changes in cells, including increases or decreases in cellular products and variations in cell morphology. Such methods also provide advantages over conventional methods, such as well-based screening,

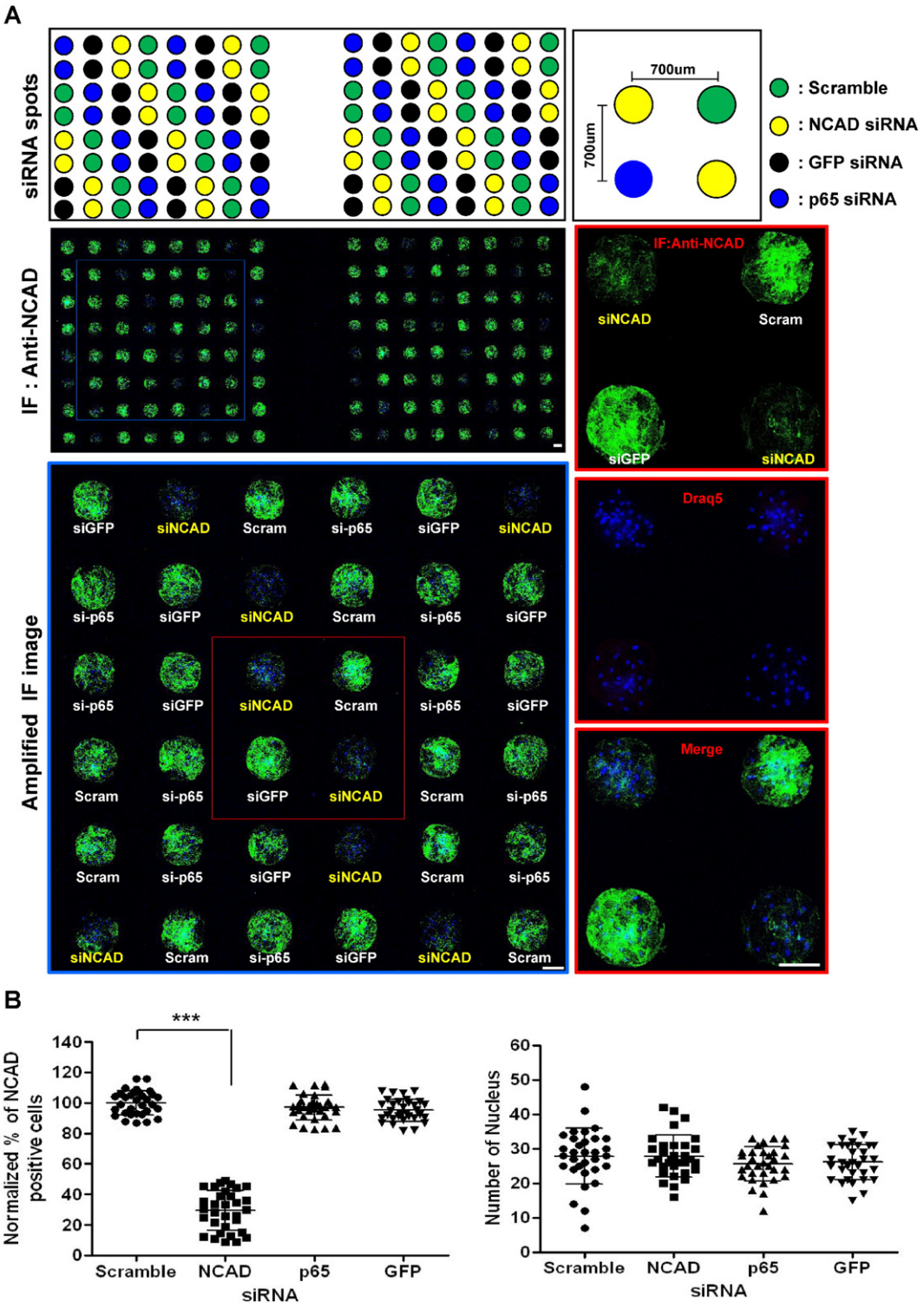

Fig. 6. The confirmation of multispot siRNA microarray quality after 48 h transfection. (A) The anti-NCAD immunofluorescence image of NCAD protein inhibited expression from the multispots of four kinds siRNA. The image shows the localization of the spots for scramble, p65, GFP and NCAD siRNA. All siRNA spots were printed in 32 spots each using two pins (for a total of 128 spots). (B) Quantitative scatter analysis and normalized results of the NCAD-positive cell ratios and cell numbers shown in (A) (representative of $n = 32$ array spots, scale bar = 100 μm). The image was acquired by an ImageXpress Ultra Point scanning confocal microscope with anti-NCAD antibodies. Blue: Draq5 for the nucleus, green: fluorescently labeled anti-NCAD antibody. Scramble siRNA was used as a control. Each error bar represents the mean ± SD. $^{***}p < 0.001$: statistical significance for the comparison with scramble siRNA.

which requires high numbers of cells, large-scale and time consuming. Indeed, our microarray system allowed the printing of up to 3888 spots per slide, permitting screening of the entire genome with only 5–7 microarray slides (Genovesio et al., 2011a, 2011b). Moreover, in our current CDSM method, we overcame the limitation of using actively mobile cells, such as hBMSCs, which were previously found to migrate outside of the spot area, spreading to other spots. Additionally, many investigators have already pursued new strategies for minimizing the spreading phenomenon in microarrays, such as poly-*N*-isopropylacrylamide (PNI) micropatterning (Zhang et al., 2011). These methods require several steps, including polymer coating and removal by controlling the temperature, and have mostly been applied in cancer cell lines, with few studies reporting hBMSC-based microarrays. It is generally considered challenging to apply mesenchymal cells to large-scale cell imaging methods for analysis of genetic functions and signal pathways using siRNA. We showed that high-efficiency, persistent siRNA knockdown could be achieved in hBMSCs, with only 30–60 cells per spot and with no requirement for additional subculture of hBMSCs. These results suggested that this approach might have applicability in a variety of assays, including screening with combinations of compounds, protein inhibitors, viruses,

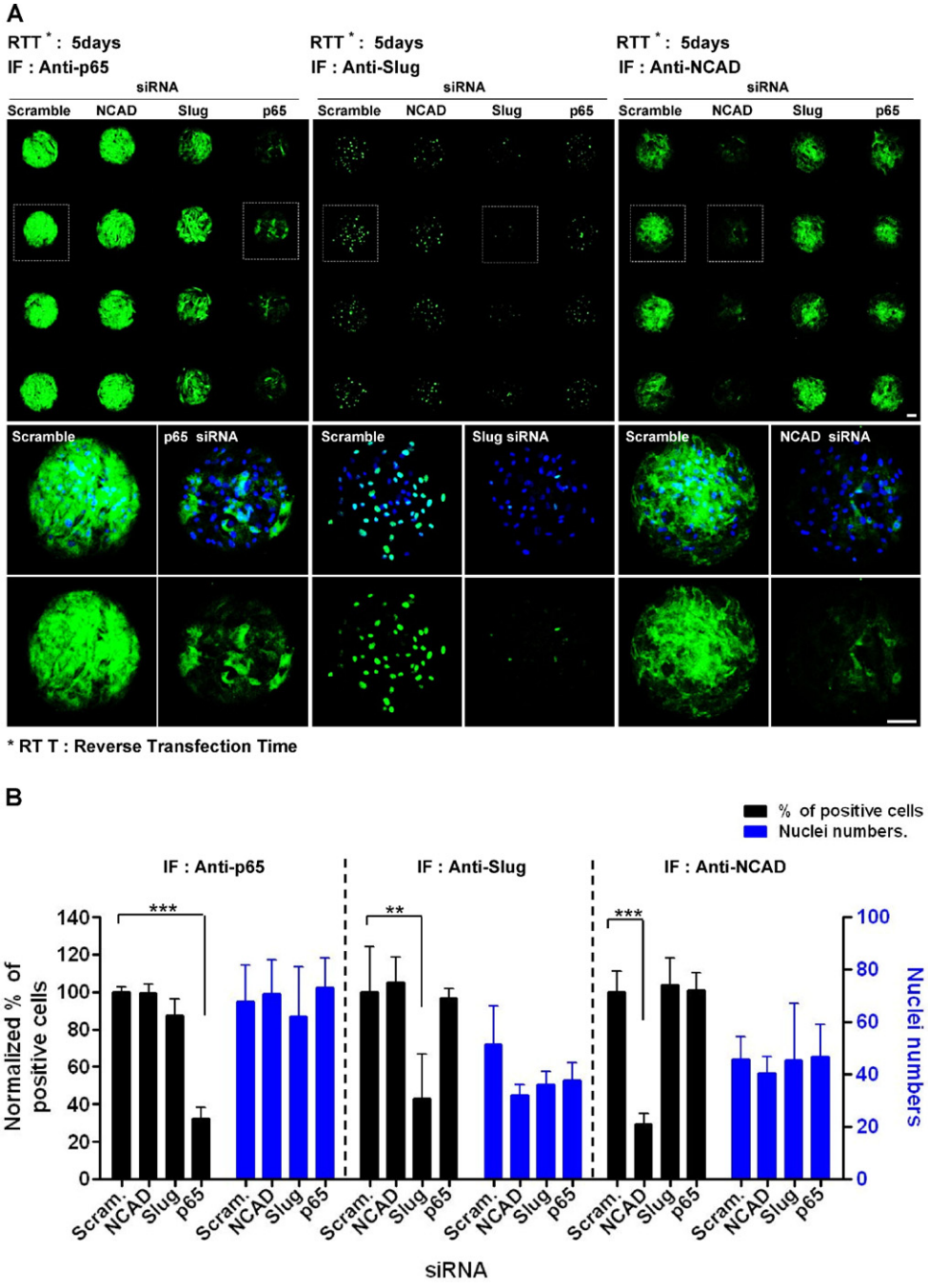

Fig. 7. Verification of the persistence of gene expression silencing. (A) Immunofluorescence images of knockdown of p65, Slug, and NCAD by siRNA after 5 days of reverse transfection. (B) Quantitative analysis of p65-, Slug-, and NCAD-positive cell ratios and cell numbers from data in (A) (lower panel) (representative of $n = 6$ array spots, scale bar = 100 μm). The images were acquired using an ImageXpress Ultra Point scanning confocal microscope with anti-p65, anti-Slug, and anti-NCAD antibodies. Blue: Draq5 for detection of nuclei, green: fluorescence-labeled antibody targeting the appropriate protein. Scramble siRNA was used as a control. The analysis was performed with MetaXpress software. Bars and error bars represent means ± SDs. $^{**}p < 0.01$, $^{***}p < 0.001$: statistical significance in comparison with scramble siRNA.

and double immunofluorescent probes. The sustained activity of printed siRNA spots (2 months when stored at 4 °C) offers opportunity for repeat screening and variations in experimental setups. Thus, this CDSM method represents a qualitatively improved siRNA microarray screening method for hBMSCs.

5. Conclusions

Gene networks in hBMSCs are critical for understanding of their function; the CDSM method for functional genomic analysis is expected to contribute for more efficient genomic research.

Acknowledgements

This work was supported by a grant from the National Research Foundation of Korea (NRF) funded by the Korean government (MSIP; grant nos. NRF-2014K1A4A7A01074642 and NRF-2013M3A9B5076486), Gyeonggi-do, KISTI, and the Korean Health Technology R&D Project , Ministry of Health and Welfare, Republic of Korea (grant no. HI12C1804).

Appendix A. Supplementary data

Supplementary data to this article can be found online at http://dx.doi.org/10.1016/j.scr.2016.02.019.

References

Baghdoyan, S., Roupioz, Y., Pitaval, A., Castel, D., Khomyakova, E., Papine, A., Soussaline, F., Gidrol, X., 2004. Quantitative analysis of highly parallel transfection in cell microarrays. Nucleic Acids Res. 32, e77.

Castel, D., Pitaval, A., Debily, M.A., Gidrol, X., 2006. Cell microarrays in drug discovery. Drug Discov. Today 11, 616–622.

Cherry, S., 2009. What have RNAi screens taught us about viral-host interactions? Curr. Opin. Microbiol. 12, 446–452.

Erfle, H., Neumann, B., Liebel, U., Rogers, P., Held, M., Walter, T., Ellenberg, J., Pepperkok, R., 2007. Reverse transfection on cell arrays for high content screening microscopy. Nat. Protoc. 2, 392–399.

Fire, A., Xu, S., Montgomery, M.K., Kostas, S.A., Driver, D., Mello, C.C., 1998. Potent and specific genetic interference by double-stranded RNA in *Caenorhabditis elegans*. Nature 391, 806–811.

Genovesio, A., Giardini, M.A., Kwon, Y.J., de Macedo Dossin, F., Choi, S.Y., Kim, N.Y., Kim, H.C., Jung, S.Y., Schenkman, S., Almeida, I.C., Emans, N., Freitas-Junior, L.H., 2011b. Visual genome-wide RNAi screening to identify human host factors required for *Trypanosoma cruzi* infection. PLoS One 6, e19733.

Genovesio, A., Kwon, Y.J., Windisch, M.P., Kim, N.Y., Choi, S.Y., Kim, H.C., Jung, S., Mammano, F., Perrin, V., Boese, A.S., Casartelli, N., Schwartz, O., Nehrbass, U., Emans, N., 2011a. Automated genome-wide visual profiling of cellular proteins involved in HIV infection. J. Biomol. Screen. 16, 945–958.

Howard, S., Deroo, T., Fujita, Y., Itasaki, N., 2011. A positive role of cadherin in Wnt/β-catenin signalling during epithelial–mesenchymal transition. PLoS One 6, e23899.

Iorns, E., Turner, N.C., Elliott, R., Syed, N., Garrone, O., Gasco, M., Tutt, A.N., Crook, T., Lord, C.J., Ashworth, A., 2008. Identification of CDK10 as an important determinant of resistance to endocrine therapy for breast cancer. Cancer Cell 13, 91–104.

Kittler, R., Pelletier, L., Heninger, A.K., Slabicki, M., Theis, M., Miroslaw, L., Poser, I., Lawo, S., Grabner, H., Kozak, K., Wagner, J., Surendranath, V., Richter, C., Bowen, W., Jackson, A.L., Habermann, B., Hyman, A.A., Buchholz, F., 2007. Genome-scale RNAi profiling of cell division in human tissue culture cells. Nat. Cell Biol. 9, 1401–1412.

Kumar, R., Conklin, D.S., Mittal, V., 2003. High-throughput selection of effective RNAi probes for gene silencing. Genome Res. 13, 2333–2340.

Luo, J., Emanuele, M.J., Li, D., Creighton, C.J., Schlabach, M.R., Westbrook, T.F., Wong, K.K., Elledge, S.J., 2009. A genome-wide RNAi screen identifies multiple synthetic lethal interactions with the Ras oncogene. Cell 137, 835–848.

Mousses, S., Caplen, N.J., Cornelison, R., Weaver, D., Basik, M., Hautaniemi, S., Elkahloun, A.G., Lotufo, R.A., Choudary, A., Dougherty, E.R., Suh, E., Kallioniemi, O., 2003. RNAi microarray analysis in cultured mammalian cells. Genome Res. 13, 2341–2347.

Prudêncio, M., Lehmann, M.J., 2009. Illuminating the host — how RNAi screens shed light on host–pathogen interactions. Biotechnol. J. 4, 826–837.

Rantala, J.K., Mäkelä, R., Aaltola, A.R., Laasola, P., Mpindi, J.P., Nees, M., Saviranta, P., Kallioniemi, O., 2011. A cell spot microarray method for production of high density siRNA transfection microarrays. BMC Genomics 12, 162.

Redmond, T.M., Ren, X., Kubish, G., Atkins, S., Low, S., Uhler, M.D., 2004. Microarray transfection analysis of transcriptional regulation by cAMP-dependent protein kinase. Mol. Cell. Proteom. 3, 770–779.

Scholl, C., Fröhling, S., Dunn, I.F., Schinzel, A.C., Barbie, D.A., Kim, S.Y., Silver, S.J., Tamayo, P., Wadlow, R.C., Ramaswamy, S., Döhner, K., Bullinger, L., Sandy, P., Boehm, J.S., Root, D.E., Jacks, T., Hahn, W.C., Gilliland, D.G., 2009. Synthetic lethal interaction between oncogenic KRAS dependency and STK33 suppression in human cancer cells. Cell 137, 821–834.

Seyhan, A.A., Ryan, T.E., 2010. RNAi screening for the discovery of novel modulators of human disease. Curr. Pharm. Biotechnol. 11, 735–756.

Silva, J.M., Mizuno, H., Brady, A., Lucito, R., Hannon, G.J., 2004. RNA interference microarrays: high-throughput loss-of-function genetics in mammalian cells. Proc. Natl. Acad. Sci. U. S. A. 101, 6548–6552.

Stürzl, M., Konrad, A., Sander, G., Wies, E., Neipel, F., Naschberger, E., Reipschläger, S., Gonin-Laurent, N., Horch, R.E., Kneser, U., Hohenberger, W., Erfle, H., Thurau, M., 2008. High throughput screening of gene functions in mammalian cells using reversely transfected cell arrays: review and protocol. Comb. Chem. High Throughput Screen. 11, 159–172.

Webb, B.L., Díaz, B., Martin, G.S., Lai, F., 2003. A reporter system for reverse transfection cell arrays. J. Biomol. Screen. 8, 620–623.

Wheeler, D.B., Carpenter, A.E., Sabatini, D.M., 2005. Cell microarrays and RNA interference chip away at gene function. Nat. Genet. 37, S25–S30.

Zhang, H., Hao, Y., Yang, J., Zhou, Y., Li, J., Yin, S., Sun, C., Ma, M., Huang, Y., Xi, J.J., 2011. Genome-wide functional screening of miR-23b as a pleiotropic modulator suppressing cancer metastasis. Nat. Commun. 2, 554.

Ziauddin, J., Sabatini, D.M., 2001. Microarrays of cells expressing defined cDNAs. Nature 411, 107–110.